Optimal Sensor Launching with UAVs for Monitoring of Hazardous Environments

André Farinha*, Salua Hamaza†, Guy Burroughes‡ and Mirko Kovac*§
*Aeronautics Department, Imperial College, London, United Kingdom, Email: a.farinha17@imperial.ac.uk
†Faculty of Aerospace Engineering, Delft University of Technology, Delft, The Netherlands
‡RACE, Robotics Applications in Challeging Environments, Culham, United Kingdom
§EMPA, Swiss Federal Laboratories for Materials Science and Technology, Zurich, Switzerland

***Abstract*—Sensor launching is an approach to remote sensor placement which can accurately deploy sensor nodes while maintaining a safe distance from obstacles, making it a promising method for hazardous environments such as nuclear facilities. Moreover, as long as the sensor's trajectory can be accurately predicted, up to ± 5 cm precision can be achieved with little on-board computation and perception. This extended abstract covers a robust method to predict said trajectories and the formulation of an optimal problem to find effective initial launching poses.**

I. Sensor deployment with UAVs

Wireless Sensor Networks (WSN) have been shown to improve data gathering processes over large spatial and temporal scales at a low cost [1], as well as the automation of decision making processes in complex industrial settings [2]. The nuclear sector is no exception to this, being potential applications structural health monitoring [3] and radiation monitoring [4]. While the greatest level of integration of such systems can be achieved during reactor construction, the nuclear energy field has an abundance of research or legacy reactors that need to be fitted with such systems as deemed necessary. The use of Unmanned Aerial Vehicles (UAVs) for such tasks is unintrusive and safe, as it can be performed remotely, and has been successfully demonstrated for different applications [5]–[7]. Here, we further propose the deployment of said networks in hazardous environments by launching the sensors from on-board a UAV towards desired targets. This method was first proposed for cluttered environments in [8] and we hereby expand on the subjects of sensor trajectory modelling and obstacle-aware optimal trajectory planning. This method is shown to be robust to densely cluttered environments using minimal perception and computational power, making it ideally suited for contained environments and narrow spaces, inaccessible to larger aerial platforms. Further contributions of this work include the real time calculation of accurate sensor launching trajectories and a method to make these trajectories invariant with changes in the sensory payload.

This work was supported by NERC and NPIF grant NE/R012229/1, and carried out within the framework of the EUROfusion Consortium, funded by the European Union via the Euratom Research and Training Programme (Grant Agreement No 101052200 — EUROfusion). Views and opinions expressed are however those of the author(s) only and do not necessarily reflect those of the European Union or the European Commission. Neither the European Union nor the European Commission can be held responsible for them. The work of Mirko Kovac is supported by the Royal Society Wolfson fellowship (RSWF/R1/18003).

II. Nuclear fusion use-case

Nuclear environments are some of the most hazardous environments in the world, driving the need for robotics and autonomous applications in the field. Particularly in nuclear fusion plants, considerable advances in remote maintenance and inspection are necessary before commercialisation is possible [9]. Serial manipulators, amongst other tools have been successfully used in maintenance of the Joint European Torus (JET), however, as facilities become larger to support larger tokamaks, the amount of space that needs to be inspected and maintained grows exponentially. For example, the proposed DEMO active maintenance facility will be used to autonomously maintain the robots that maintain the fusion reactor, and will span 737,000m^3 all requiring remote inspection and intervention for maintenance [10]. UAVs can not only enable the inspection of such locations, but also their medium to long term monitoring, if sensor nodes are deployed. The capacity to launch these sensors is exacerbated when taking into account the dense clutter in these locations, as hazardous flight in close proximity to solid objects is not necessary.

III. Robust sensor trajectory prediction

The precision of sensor launching methods is a combination of the UAV's position control, accumulated error from the sensor's trajectory, and change in pose resulting form the launch. While the first is a problem that is generic to UAV control, the following 2 are particular to sensor launching.

There are two main sources of uncertainty in the trajectory of low Reynolds projectiles[1] such as small sensors: 1) the drag of the sensor, which is typically a bluff body[2] and thus subject to large variability, incoming turbulence and sensor shape; 2) the pitch and yaw oscillations, which have the effect of momentarily increasing drag, leading to shorter ranges than expected, but also to somewhat random deviations from predicted trajectories. The accurate prediction of such trajectories would normally be achieved by fully characterising projectile aerodynamics by numerically solving the Navier-Stokes equations, or empirically via wind tunnel experiments. However, relying on such computationally intensive methods would limit the variety of usable payloads. To this purpose,

[1]low Re flows are characterised by low speeds around small sized objects
[2]non aerodynamically shaped objects such as cuboids

we employ a different strategy, where we compromise in accuracy, and aim instead for obtaining similarity in behaviour of various sensor payloads and then deploy reduced order models. The first step towards this objective consists in sizing a tail stabiliser for the projectile such that the half-life of pitch oscillations meet a certain target value. As such, a reduced model where pitch oscillations are neglected can be used, and the resulting excess drag can be empirically estimated. Initial conditions, pitch perturbations and aerodynamic coefficients such as bluff body drag, can also be optimised to better fit experiments. Finally, validation against experiments provides a confidence interval on the trajectory prediction as function of travelled distance and initial conditions.

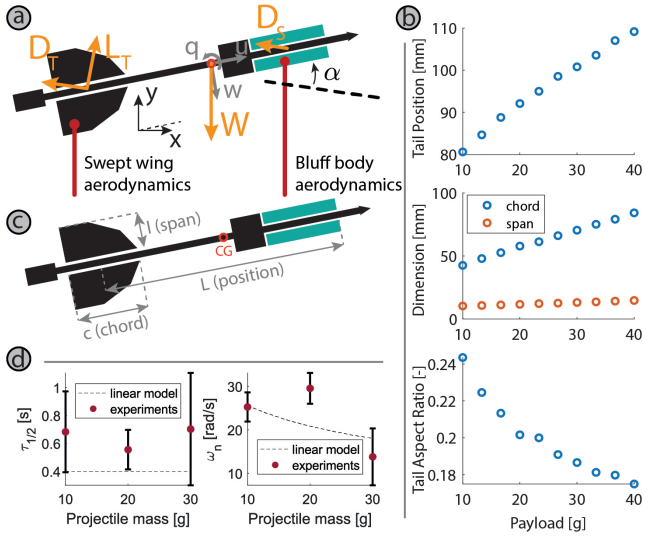

Fig. 1. A. Projectile geometry and applied forces. B. Optimised stabiliser geometry for different payloads. C. Stabiliser geometrical parameters, D. Experimental verification of damping parameters predicted by optimisation problem

The planar dynamics of an object in fight are given by eqs. (1) and (2) where F_u, F_w and M_v are the projections of the forces shown in fig. 1a on the body frame. These equations can be linearised in the form of eq. (3), where $\mathbf{A}$ is obtained from the slope of the aerodynamic force coefficients, $\mathbf{x}$ corresponds to the state vector $[u\, w\, q\, \theta]$ defined in fig. 1a, and $\dot{\mathbf{x}}$ its derivative (note that $\dot{\theta} = q$). The oscillatory behaviour of a projectile is then estimated by solving this eigenvalue problem.

$$\begin{bmatrix} F_u \\ F_w \\ M_v \end{bmatrix} = \begin{bmatrix} m & & \\ & m & \\ & & I_{yy} \end{bmatrix}_{diag} \left(\begin{bmatrix} \dot{u} \\ \dot{w} \\ \dot{q} \end{bmatrix} + \begin{matrix} q & w \\ q & u \\ & \end{matrix} \right) \tag{1}$$

$$\begin{bmatrix} \dot{x} \\ \dot{z} \\ \dot{\theta} \end{bmatrix} = R \begin{bmatrix} u \\ w \\ q \end{bmatrix} \tag{2}$$

$$\dot{\mathbf{x}} = \mathbf{A}_{4;4}\ \mathbf{x} \tag{3}$$

The optimisation problem defined in eq. (4) finds aft tail dimensions that ensure the same oscillatory motion decay for different payload mass and shapes. Figure 1b shows the obtained tail geometrical parameters for a $\tau_{1=2(tg)} = 0.4$, where $\tau_{1=2}$ is the time it takes for the amplitude of pitch oscillations to reduce by $1/2$. The design space is in the tail's $(chord, span, position)$, defined in fig. 1c and minimisation is for the relative error of the target half-life (e.g. 0.4), and total mass to payload mass ratio. The system is ensured to be over-damped by applying a lower barrier function (lbf) to entry (3,2) in $\mathbf{A}$ (eq. (3)) respective to $\partial C_M/\partial\alpha \overset{!}{?} \partial C_M/\partial w$. It's shown in fig. 1d that this exercise is partially successful in ensuring self-similar behavior between projectiles of different masses. The greatest source of experimental variability is the initial launching angle, between 5 and 80 degrees, which introduces variability in the second order terms in eq. (1).

$$\min \quad \frac{\tau_{1=2(tg)} \quad \tau_{1=2}}{\tau_{1=2}} + \frac{m_t}{m_p} + lbf(\mathbf{A}_{(3;2)}) \tag{4}$$

After similarity in pitch oscillations is ensured, the pitch DoF is removed, and the projectile can be treated as a point mass subject to drag. Rearranging eq. (1) into tangential ($\underline{u}$) and normal ($\dot{\theta}$) coordinates and assuming $x(t)$ to be invertible, the system of equations 5 is obtained, which is dependent on x instead of t. This has the advantage that the problem can be treated as a boundary value problem (BVP), allowing us to set impact conditions and infer a launch position.

A limitation on the rationale discussed thus far is that the vast majority of viscous drag losses at low Re numbers 10^4 are not due to the drag term D_0 at zero α, but due to large pitch oscillations. We hypothesise that these oscillations are induced in the trajectory due to the lag between the projectile's inertia and gravity induced trajectory curvature. The term $\frac{D}{u^2}\frac{g}{}$ in eq. (5b) is introduced as a drag term proportional to the curvature of the trajectory $\frac{d}{dx}$.

$$\frac{dz}{dx} = \tan\theta \tag{5a}$$

$$\frac{du}{dx} = \frac{-g\sin\theta \quad \frac{1}{m}D_0}{u\cos\theta} \quad \frac{D}{u^2}\frac{g}{} \tag{5b}$$

$$\frac{d\theta}{dx} = -\frac{g}{u^2} \tag{5c}$$

IV. Optimal Sensor Launching

Depending on the launching mechanism on-board, the solution of eq. (5) can be singular or not. This is the case if the launch energy or (as in section V), the initial launch pitch can be controlled. In this case, an optimisation problem can be defined to obtain advantageous solutions in terms of distance to obstacles or impact conditions.

Considering quasi-stationary conditions during launch, we have 5 dof deriving from the multirotor's pose $\mathbf{x_0}$ and the launcher's inclination θ_0, for 3 dof constraining the target's position $\mathbf{x_{trg}}$. Even after reducing the problem to the plane, there's an infinite number of possible solutions, however, an optimal problem can be solved in terms of criteria such as

placement accuracy, distance to clutter, etc. Here, we simplify this problem by reducing it to 2D, however, the same approach can be used if considerably more effort is taken in clutter detection using more complex sensing and visual processing.

Besides ensuring placement in a desired location, sensor launching in cluttered environments needs to take into account the proximity of obstacles to the multicopter and potential trajectories. Optionally, the size of the target relative to the confidence interval on the trajectory, the impact energy and impact angle to target surface can also be taken into account. Equations 5 are solved as a black-box model and the mentioned objectives and constraints are introduced in the objective function as in eq. (6), and normalised. Where $\mathbf{x_{trg}}$, $\theta_?$ and L_{trg}, correspond respectively to the target position, target surface normal and target characteristic dimension.

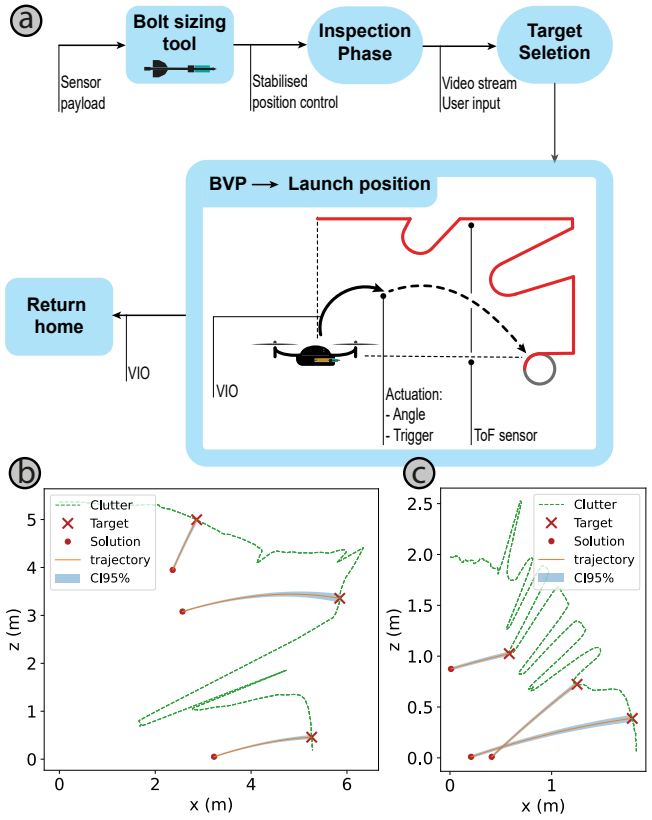

Fig. 2. A. Operations flowchart from selection of a sensor payload operator flight and target selection and optimal launching. B,C. Launch position optimisation results in environments with pipes of ∼10 cm diameter. CI95% corresponds to the 95% confidence interval on the predicted optimal trajectory.

Taking into account target facilities in the JET, we consider that we will be targeting mostly either straight walls or pipelines between 20 and 50 cm diameter. In order to find which of these cases is in occurrence and which wall/tube best fits the region surrounding the environment, a least squares problem is formulated and the case with lowest residual chosen. These problems are defined with the impact point as the center of the reference frame and thus the first case is defined using a single parameter - the slope angle of a line in polar coordinates, and for the second case two parameters - the center of a circle in Cartesian coordinates. Jacobians are easily calculated from the expressions derived this way.

$$min(jj\mathbf{x_i} \quad \mathbf{x_{trg}}jj) \tag{6a}$$

$$min(j\theta_i \quad \theta_?j) \tag{6b}$$

$$\int_0^{\mathbf{x_i}} R_{clutter} \quad ((\mathbf{x} \quad [0, CI_{95\%}])_{\underline{r}})_1 \, d\theta \tag{6c}$$

Given eq. (5) is defined in space, this problem can be defined in a direct way (3-dimensional optimisation space: $\mathbf{x}$, θ_0) or inverse (2 dimensional space: θ_i, K_{E_i}). Both formulations are solved using global optimisers, because convexity cannot be ensured. Simulations results are shown in fig. 2b,c for real indoors and outdoors scenarios described by data obtained with the on-board sensors.

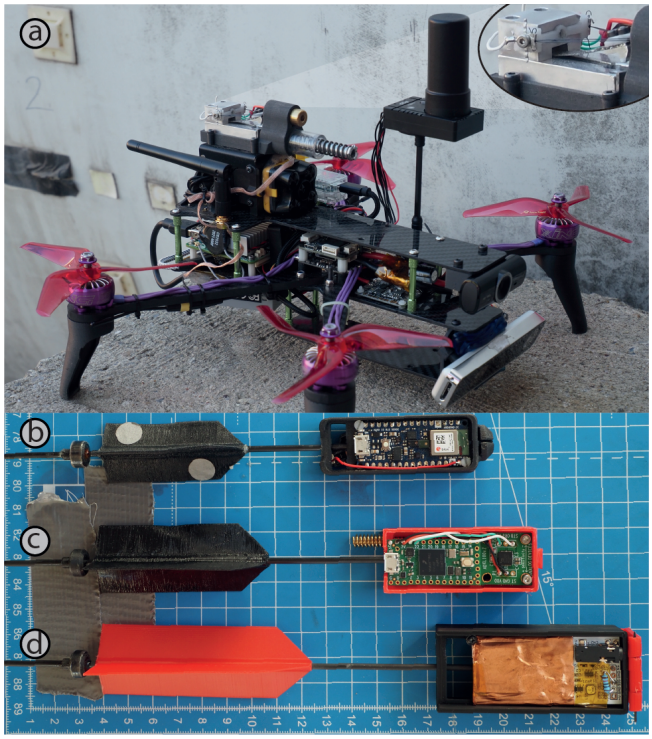

Fig. 3. A. Multicopter and sensor launching system used in experiments. B. 15g sensor for leak detection. C. 21g sensor used in condition monitoring. D. 29g sensor used in radiation monitoring.

V. System Design

The sensor launcher shown in fig. 3a is based on the one presented in [8], which uses an SMA for actuation of the sear catch, however, the mechanism is updated to have the sear integrated into the spring to facilitate sensor manufacturing. The launcher is mounted on a servo-motor (*DYNAMIXEL XC330-M288-T 2021*) and integrated on a custom 5.1" quadcopter frame. An infra-red time-of-flight sensor with 2 field of view (*TeraRanger Evo 60m 2021*) is mounted on the servomotor and